J Physiol Sci (2016) 66:477–490
DOI 10.1007/s12576-016-0443-6

ORIGINAL PAPER

Different rate-limiting activities of intracellular pH regulators for HCO_3^- secretion stimulated by forskolin and carbachol in rat parotid intralobular ducts

Kaori Ueno[1] · Chikara Hirono[1] · Michinori Kitagawa[1] · Yoshiki Shiba[1] · Makoto Sugita[1]

Received: 19 October 2015 / Accepted: 23 February 2016 / Published online: 11 March 2016

Abstract Intracellular pH (pH_i) regulation fundamentally participates in maintaining HCO_3^- release from HCO_3^--secreting epithelia. We used parotid intralobular ducts loaded with BCECF to investigate the contributions of a carbonic anhydrase (CA), anion channels and a Na^+–H^+ exchanger (NHE) to pH_i regulation for HCO_3^- secretion by cAMP and Ca^{2+} signals. Resting pH_i was dispersed between 7.4 and 7.9. Forskolin consistently decreased pH_i showing the dominance of pH_i-lowering activities, but carbachol gathered pH_i around 7.6. CA inhibition suppressed the forskolin-induced decrease in pH_i, while it allowed carbachol to consistently increase pH_i by revealing that carbachol prominently activated NHE via Ca^{2+}-calmodulin. Under NHE inhibition, forskolin and carbachol induced the remarkable decreases in pH_i, which were slowed predominantly by CA inhibition and by CA or anion channel inhibition, respectively. Our results suggest that forskolin and carbachol primarily activate the pH_i-lowering CA and pH_i-raising NHE, respectively, to regulate pH_i for HCO_3^- secretion.

Keywords Intracellular pH · Rat parotid intralobular ducts · Bicarbonate secretion · Na^+–H^+ exchanger · Carbonic anhydrase · Cl^- channels

✉ Chikara Hirono
chikara@hiroshima-u.ac.jp

[1] Department of Physiology and Oral Physiology, Institute of Biomedical and Health Sciences, Hiroshima University, 2-3 Kasumi 1-Chome, Minami-ku, Hiroshima 734-8553, Japan

Introduction

Salivary glands are formed by acinar and ductal parts. Acini secrete the plasma-like, isotonic fluid "primary saliva", whereas ducts modify the saliva components by secretion of HCO_3^- and K^+ as well as reabsorption of Na^+ and Cl^- [1–3]. The volume of saliva induced by the Ca^{2+} signal is much larger than that by the cAMP signal in vivo and ex vivo [4, 5]. Most of the salivary fluid is secreted by acinar parts. However, it is suggested that both signals also induce fluid secretion from ductal parts, which accompanies HCO_3^- release [6, 7]. Secretion of the appropriate concentration of HCO_3^- is an important function of the ducts to keep oral health by means of the pH buffering effect of HCO_3^- [2, 3]. Several models were proposed for mechanisms of HCO_3^- secretion from salivary ducts, corresponding to divergence among animal species, types of salivary glands, and parts of the salivary ducts [2, 6, 8–10]. The relative amount of secreted HCO_3^- also depends on the divergence. A parasympathomimetic Ca^{2+}-mobilizing agonist (carbachol; CCh) and a sympathomimetic cAMP-increasing agonist (isoproterenol) stimulate HCO_3^- secretion in the main excretory duct of rat submandibular glands [11]. In rat parotid glands, there is no report about HCO_3^- secretion in the main excretory duct and expression levels of factors involved in HCO_3^- secretion in each part of the duct is unknown. However, HCO_3^- secretion evoked by forskolin, a cAMP-increasing agent, and CCh in the rat parotid intralobular ducts is clearly demonstrated in the cell and tissue levels [6, 7, 12]. The intracellular pH (pH_i) regulation plays an important role in keeping HCO_3^- secretion. Therefore, in this paper, we focused on the mechanism of pH_i regulation during HCO_3^- secretion in the rat parotid intralobular ducts. In a proposed model for the rat parotid intralobular duct, intracellular HCO_3^- is

generated by the cooperative activities of carbonic anhydrases (CA) and Na^+–H^+ exchangers (NHE) [6, 12]. HCO_3^- is released through Cl^- channels in the model. One of the channels is a CFTR Cl^- channel mainly dependent on the cAMP signal [7, 12], as reported in the submandibular ducts [13, 14]. The other is a diphenylamine-2-carboxylate (DPC)-sensitive Cl^- channel apparently activated by the Ca^{2+} signal [6, 15] and this channel has not yet been identified. The amplitude of inward currents evoked by the cAMP signal is around 75 pA at the membrane potential of −80 mV in the single cells of rat parotid intralobular ducts [12]. Removal of external HCO_3^- and CO_2 reduces these currents, indicating that the currents reflect HCO_3^- secretion [12]. The Ca^{2+} signal also elicits the HCO_3^-- and CO_2-dependent currents with the amplitude similar to those induced by the cAMP signal (unpublished data). The rate of HCO_3^- secretion is determined by the activities of the HCO_3^--releasing Cl^- channels, NHE and CA, which appear to cooperatively maintain and regulate pH_i. However, the relative contribution of those activities to the pH_i regulation and HCO_3^- secretion induced by cAMP and Ca^{2+} signals remains elusive.

Among the NHE isoforms expressed in salivary glands, NHE1 located in the basolateral membrane mainly regulates the pH_i in mouse parotid and sublingual acinar cells [16, 17] and in rat parotid acinar cells [18]. In rat parotid ductal cells, the basolaterally-located NHE1 and apically-located NHE3 are concerned with regulation of pH_i [18]. Nevertheless, NHE3 located in the apical membrane of mouse parotid ductal cells does not play a major role in Na^+ absorption [19]. Moreover, physiological function of NHE3 that is sensitive to cAMP-mediated inhibition [20] remains unclear in rat submandibular gland ducts [21]. It is very likely that NHE1 is the functionally relevant NHE isoform in parotid ductal cells.

There are many reports about pH_i regulation by NHE and the mechanisms of NHE activation in various organs. Osmotic cell shrinkage causes an alkaline shift in the pH_i set point of NHE in resident alveolar macrophages [22]. NHE1 is active during metabolic inhibition in rabbit ventricular myocytes if pH_i is driven more acidic than NHE1 set-point pH_i [23]. Ca^{2+}-calmodulin activates NHE1, and the calmodulin-binding autoinhibitory domain controls "pH-sensing" in NHE1 expressed in the exchanger-deficient cell PS120 [24, 25]. On the other hand, MAP kinase-dependent phosphorylation is involved in the regulation of NHE in the rat myocardium [26]. In parotid acinar cells, CCh induces phosphorylation-independent activation of NHE1 [27]. There may exist some processes, such as association of Ca^{2+}-calmodulin complexes to the cytosolic domain of NHE1 during CCh stimulation [27], as reported for the cultured cells. However, the detailed mechanism of NHE activation in salivary glands, especially in ductal cells, is still unknown.

Carbonic anhydrase isozymes I, II and VI (CAI, CAII and CAVI) are localized in rat parotid glands [28, 29], whereas CAVI is secreted into saliva [29]. It is reported that an increase in the intracellular cAMP concentration activates CAIX through phosphorylation at the intracellular domain by the protein kinase A in hypoxia in cultured cell lines [30]. However, the activation mechanism of the CA isozymes expressed in salivary glands during the cAMP signaling has not yet been reported.

In this paper, we characterized the regulatory mechanisms of pH_i in rat parotid intralobular ductal cells stimulated by forskolin and CCh, and investigated which factor, the Cl^- channel, NHE or CA, has the rate-limiting activity for pH_i regulation and HCO_3^- secretion induced by each of cAMP and Ca^{2+} signals. Although there may be a cross-talk between cAMP and Ca^{2+} signals, the results obtained suggest that forskolin-induced cAMP signals and CCh-induced Ca^{2+} signals have different primary ways of pH_i regulation controlling mainly CA and NHE activities, respectively, during HCO_3^- secretion.

Materials and methods

Preparation of intralobular duct segments from rat parotid glands

Male Wistar rats were purchased from Charles River Laboratories Japan (Yokohama, Japan). The animal use protocol was approved by the Committee of Animal Experimentation, Hiroshima University. Parotid glands were removed from the rats (250–400 g) anesthetized with sodium pentobarbital (somnopentyl, 70–100 mg/kg, i.p.). The minced glands were digested for 45 min at 37 °C with collagenase S-1 (1 mg/ml) dissolved in a modified Krebs–Henseleit Ringer solution (KHR: 103 mM NaCl, 4.7 mM KCl, 2.56 mM $CaCl_2$, 1.13 mM $MgCl_2$, 25 mM $NaHCO_3$, 1.15 mM NaH_2PO_4, 2.8 mM glucose, 4.9 mM Na-pyruvate, 2.7 mM Na_2-fumarate, 4.9 mM Na-glutamate, 12.5 mM HEPES, pH 7.4). KHR was gassed with 95 % O_2 + 5 % CO_2 before each experiment. The digestives were dispersed by pipetting to separate intralobular duct segments from acini and washed with KHR twice.

Chemicals

Carbamylcholine chloride (carbachol, CCh), EDTA and trypsin were obtained from Nacalai Tesque (Kyoto, Japan), and collagenase (type S-1) and sodium pentobarbital (somnopentyl) were from Nitta Gelatin (Osaka, Japan) and Kyoritsu Seiyaku (Tokyo, Japan), respectively. Diphenylamine-2-carboxylate (DPC) and forskolin were purchased from Wako Pure Chemical Industries (Osaka, Japan).

Bovine serum albumin fraction V (BSA), 5(*N*,*N*)-dimethyl amiloride (DMA), gramicidin D, 3-isobutyl-methylxantine (IBMX), methazolamide, nigericin, and poly-L-lysin were obtained from Sigma-Aldrich (St. Louis, MO, USA). 1,2-Bis(2-aminophenoxy)ethane-*N*,*N*,*N*′,*N*′-tetraacetic acid, tetraacetoxymethyl ester (BAPTA-AM) and 3′-*o*-acetyl-2′,7′-bis(carboxyethyl)-4 or 5-carboxyfluorescein, diacetoxymethyl ester (BCECF-AM) were obtained from Dojindo Laboratories (Kumamoto, Japan). CFTR inhibitor 172 and W-7 hydrochloride were purchased from Calbiochem (EMD Biosciences, La Jolla, CA, USA, and EMD Chemicals, San Diego, CA, USA).

Measurement of intracellular pH in the duct segments

The duct segments were incubated for 15 min at 37 °C in KHR containing the pH-sensitive fluorescence dye BCECF-AM (0.3 μM) and 0.1 % BSA. In the experiments for intracellular Ca^{2+} chelation, 50 μM BAPTA-AM was added to the incubation medium. Then, the duct segments were washed with KHR and allowed to adhere on cover slips coated with poly-L-lysin. The ducts placed in the chamber were continuously perfused with bathing solutions, basically KHR, gassed with 95 % O_2 + 5 % CO_2. The intracellular pH (pH_i) measurement was performed by using the image analysis equipment ARGUS-HiSCA system (Hamamatsu Photonics, Hamamatsu, Japan) with the inverted microscope TE300 (Nikon, Tokyo, Japan) at room temperature (23–26 °C). The ratio of fluorescence excited at 490 nm to that at 450 nm (F490/F450) was calculated at 10-s intervals. pH_i calibration was performed based on the linear relationship between F490/F450 and pH_i in the ducts perfused with pH standard solutions (5 mM NaCl, 55 mM KCl, 85 mM K-gluconate, 0.8 mM $MgSO_4$, 10 mM HEPES, and 5 μM nigericin, pH 6.8, 7.2 or 7.6). pH_i at the 10–30 regions with the size similar to a cell in each duct was averaged and then expressed as a mean ± SE at each measurement time. These data were used for presenting the time course of pH_i change. For statistical analyses, the average pH_i was determined in the final 1 min before the addition of the agents for the resting state and from 4 to 5 min after the agent addition (or from 9 to 10 min after the DMA addition), and then expressed as mean ± SE of at least 5 experiments. The statistical difference was regarded as significant when $P < 0.05$ by using paired or unpaired Student's *t* test.

Ionic current measurements in the ductal cells

Dispersed parotid glands, obtained by the collagenase treatment and pipetting, were poured into a 90-mm dish to allow the duct segments to adhere tightly to the dish. Acini in the dish were roughly washed out with KHR. The ducts still attaching on the dish were taken off by pipetting in 0.05 % trypsin + 0.016 % EDTA dissolved in phosphate-buffered saline, immediately collected and washed with KHR. The ducts obtained were digested again with 0.16 % collagenase (type S-1) at 37 °C for 25 min and dispersed by pipetting. The ductal cells were washed with KHR, placed on poly-L-lysine-coated cover slips and used for patch clamp experiments.

The gramicidin-perforated patch techniques were used for measuring the ionic currents from the ductal cells with a patch/whole-cell clamp amplifier CEZ-2400 (Nihon Kohden, Tokyo, Japan). Patch pipettes were pulled from borosilicate glass capillaries. The pipette solution containing 150 mM KCl, 10 mM HEPES and 0.1 mg/ml gramicidin D was adjusted to pH 7.4 using KOH. The bathing solution (KHR solution) was constantly perfused in a chamber. KHR was gassed with 5 % CO_2 + 95 % O_2. To eliminate K^+ currents, the membrane potential was held at −80 mV, which was approximately equal to the equilibrium potential of K^+. All measurements were performed at room temperature (23–27 °C). Other details of the gramicidin-perforated patch techniques were similar to those in the previous papers [12, 31].

Results

Forskolin + IBMX-induced pH_i changes and effects of methazolamide and CFTR inhibitor 172 on the responses

We previously reported that forskolin + IBMX (F+I) induces HCO_3^- generation by the carbonic anhydrase (CA) and Na^+–H^+ exchanger (NHE) system, and HCO_3^- release through the CFTR Cl^- channel in rat parotid intralobular ductal cells [7, 12]. To sustain the HCO_3^- secretion via Cl^- channels, the intracellular HCO_3^- concentration above its electrochemical equilibrium value are maintained by extrusion of H^+ by NHE, and generation of H^+ and HCO_3^- by CA. Thus, the pH_i are determined by the pH_i-raising NHE activity and the pH_i-lowering activities of CA and Cl^- channels. In the present study, we examined which factors were dominantly involved in the pH_i regulation during HCO_3^- secretion. The resting pH_i level in 9 ducts tested was distributed between 7.44 and 7.74 (7.62 ± 0.05, $n = 9$). Although variability in the resting pH_i was observed, application of F+I decreased pH_i from the resting level in all the ducts tested (Fig. 1a). F+I-induced pH_i changes (ΔpH) were correlated with the resting pH_i, showing the tendency toward gradually increasing the pH_i changes as the resting pH_i became higher (Fig. 1b). There

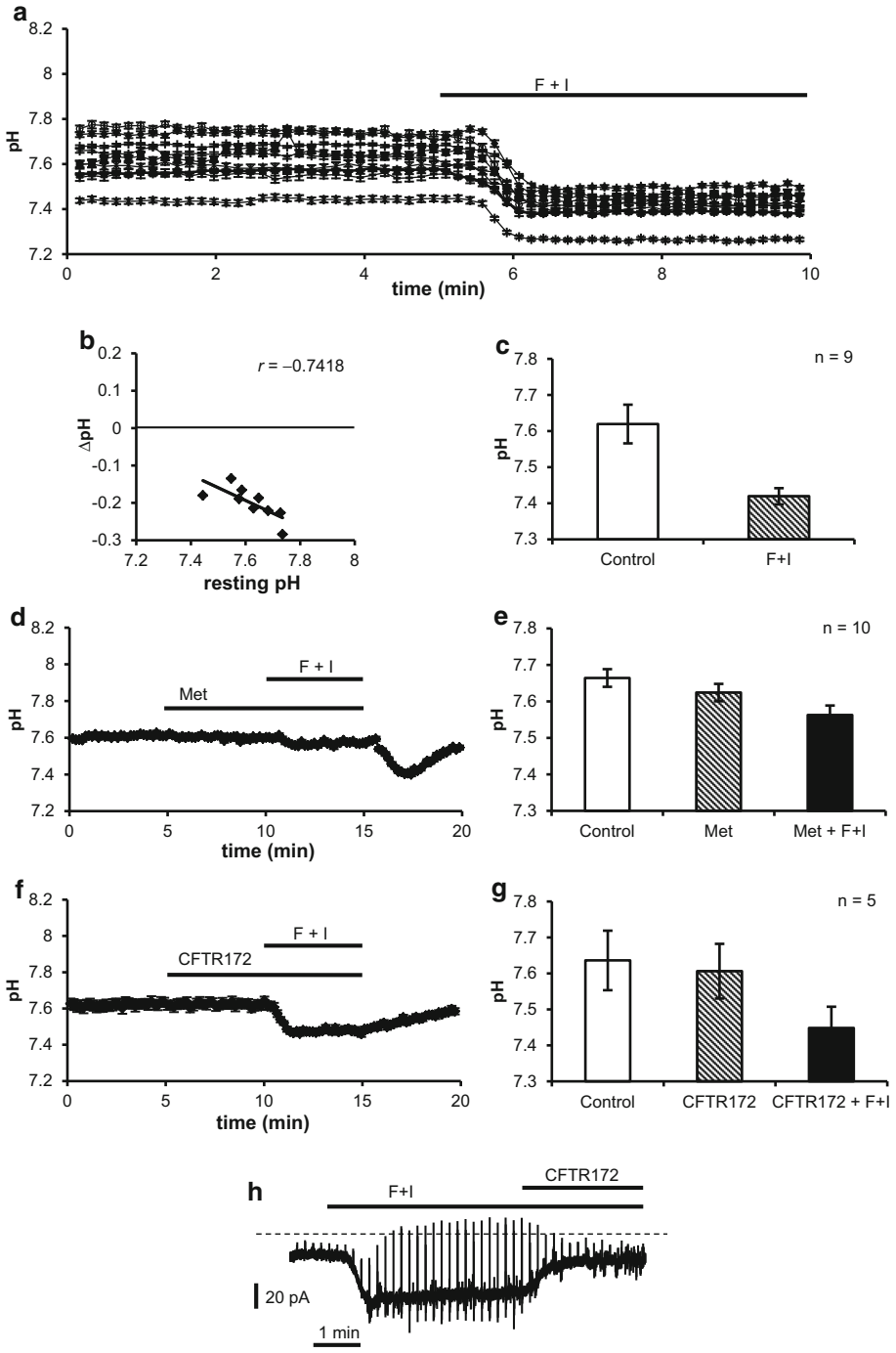

was a statistically marked difference between pH_i levels in the resting state and during the F+I stimulation (Fig. 1c; $P < 0.001$ in the paired Student's t test). The F+I-induced decrease in pH_i was significantly suppressed by pre-addition of the CA inhibitor, methazolamide (Fig. 1d, e), comparing the data shown in Fig. 1e (Met + F+I; pH_i 7.56 ± 0.03, $n = 10$) with those in Fig. 1c (F+I; pH_i 7.42 ± 0.02, $n = 9$) ($P < 0.001$ in the unpaired Student's t test). This indicates that H^+ production by some isozymes of CA contributes to the F+I-induced decrease in pH_i. F+I induces HCO_3^- release via CFTR Cl^- channels [12], which would be expected to reduce the pH_i level. However, the F+I-induced pH_i change was not affected by the presence of CFTR inhibitor 172, a potent inhibitor of the CFTR Cl^- channel [32] (Fig. 1f, g; pH_i 7.45 ± 0.06, $n = 5$). We confirmed the effectiveness of CFTR inhibitor 172 in the ductal cells by measuring F+I-induced inward currents. The inhibitor almost completely blocked the

◀**Fig. 1** Forskolin + IBMX-induced decrease in the pH_i. **a** Time courses of the pH_i changes in rat parotid intralobular ducts by the addition of 10 μM forskolin + 100 μM IBMX (F+I). Each *point* indicates the mean ± SE of pH_i in 19–28 regions of the ducts. The pH_i level was reduced by the addition of F+I in all the ducts tested. **b** Relationships between the F+I-induced pH_i changes averaged during 4–5 min after F+I addition (ΔpH) and the resting pH_i levels averaged for 1 min just before F+I addition. Each *point* was obtained from the data in **a** ($n = 9$). **c** The pH_i averaged for 1 min just before F+I addition (control) and 4–5 min after F+I application (F+I). Data shown are mean ± SE calculated from the traces in **a** ($n = 9$). **d** A time course of pH_i change in the duct by F+I addition of under the inhibition of carbonic anhydrases by 1 mM methazolamide (Met). Each *point* indicates the mean ± SE of pH_i in 20 regions of the duct. **e** The effect of 1 mM methazolamide on the F+I-induced pH_i change. The pH_i averages for 1 min just before (control, pH_i; 7.57–7.83) and 4–5 min after (Met) the addition of methazolamide, and 4–5 min after the subsequent addition of F+I (Met + F+I) are denoted. Data shown are mean ± SE ($n = 10$). **f** A time course of pH_i change in the duct by F+I addition under the blocking of CFTR Cl^- channels by 10 μM CFTR inhibitor 172 (CFTR172). Each *point* indicates the mean ± SE of pH_i in 17 regions of the duct. **g** The pH_i averages for 1 min just before (control, pH_i; 7.39–7.91) and 4–5 min after the addition of the CFTR inhibitor (CFTR172), and 4–5 min after the subsequent addition of F+I (CFTR172 + F+I) are shown. Data shown are mean ± SE ($n = 5$). **h** Addition of 10 μM CFTR inhibitor 172 (CFTR172) almost completely blocked the inward current induced by 10 μM forskolin + 100 μM IBMX (F+I). The current was measured by using the gramicidin-perforated patch techniques in a single ductal cell. Small and brief voltage pulses (5 mV, 0.2 s) were superimposed on the holding potential (−80 mV) in every 10 s. The *broken line* indicates the zero level of the current. Similar results were obtained in the other 4 experiments

currents (Fig. 1h). These results suggest that the F+I-induced decrease in pH_i may be due to the CA activity, which is functionally dominant in pH_i regulation, rather than the CFTR Cl^- channel, and that the pH_i-lowering CA activity may dominate over the pH_i-raising NHE during F+I stimulation.

F+I-induced pH_i changes under the inhibition of NHE

To further characterize the contributions of NHE, CA, and CFTR Cl^- channels to pH_i regulation during F+I stimulation, we deduced and analyzed the pH_i changes mediated by the CA and CFTR Cl^- channel activities under NHE inhibition by 5(*N*,*N*)-dimethyl amiloride (DMA). Application of DMA alone significantly decreased the pH_i (Fig. 2a, b), suggesting that NHE may be activated in the resting state. Addition of F+I in the presence of DMA induced a more remarkable decrease in pH_i (Fig. 2a, b; ΔpH_i 0.61) than did F+I alone (Fig. 1a, c; ΔpH_i 0.20). Application of DMA that inhibits the pH_i-raising NHE activity allows the pH_i-lowering activities to be profoundly unveiled. The difference in the F+I-induced ΔpH_i between the presence and absence of DMA implies that NHE is further activated during F+I stimulation, compared with that in the resting state. However, the pH_i-raising NHE might be passively activated following the F+I-induced activation of the pH_i-lowering CA and CFTR Cl^- channels, since F+I alone decreased the pH_i, and the pH_i value during F+I stimulation in the presence of methazolamide was not greater than that in the initial resting level. In the presence of CFTR inhibitor 172 or methazolamide with DMA, F+I induced a decrease in pH_i to the same level as that during F+I stimulation with DMA alone [Fig. 2a, b (DMA + F+I); pH_i 6.97 ± 0.05 ($n = 6$); Fig. 2c, d (DMA + CFTR172 + F+I); pH_i 7.02 ± 0.05 ($n = 7$); and Fig. 2e, f (DMA + Met + F+I); pH_i 7.00 ± 0.04 ($n = 6$)]. Judging from the F+I-induced ΔpH_i, both CFTR inhibitor 172 and methazolamide seem to inhibit the F+I-induced ΔpH_i in the presence of DMA in appearance. However, no difference among those three pH_i levels reached during F+I stimulation could be due to the presence of the lowest limit of pH_i in those conditions. Therefore, in the case in which the pH_i values just before the application of F+I are varied because of any effects of pre-added inhibitors, it is considered that the values of F+I-induced ΔpH_i are not suitable to evaluate and compare the effects of inhibitors on F+I-induced pH_i regulation. The pH_i level in the presence of DMA and methazolamide (Fig. 2f; pH_i 7.31 ± 0.05, $n = 6$) was lower than that in the presence of DMA only (Fig. 2b; pH_i 7.58 ± 0.04, $n = 6$), or DMA and CFTR inhibitor 172 (Fig. 2d; pH_i 7.59 ± 0.07, $n = 7$). Therefore, to evaluate the contributions of CA and Cl^- channels to the pH_i changes during F+I stimulation, here we calculated the rate of pH_i change per 10 s, $-\Delta pH/10$ s. This rate should reflect the combined influences of HCO_3^- release through Cl^- channels, and generation of H^+ and HCO_3^- by CA under the inhibition of NHE-mediated H^+ extrusion. The maximal rate of F+I-induced pH_i change in the presence of DMA was 0.105 ± 0.009/10 s, $n = 6$, and slowed by the pre-addition of methazolamide (0.039 ± 0.004/10 s, $n = 6$) more prominently than that by the CFTR inhibitor 172 (0.069 ± 0.012/10 s, $n = 7$) (Fig. 2g). Nevertheless, since the maximal rate of F+I-induced pH_i change may be affected by pH_i levels, we also calculated the rate at the constant pH_i of 7.27 in each condition to evaluate the contribution of CA and CFTR Cl^- channels to pH_i regulation. The pH_i value, 7.27, was determined, considering the data during F+I stimulation in this section and those during CCh stimulation in a later section. pH_i and $-\Delta pH/10$ s were averaged, respectively, at each sampling time during F+I stimulation in the ducts (Fig. 3a–c). Average of $-\Delta pH/10$ s at pH_i of 7.27 was calculated by linear interpolation between two data points, as is indicated by an arrow in each figure, and shown in Fig. 3d. Relative amplitude of the rate in each condition was similar to that of the maximal rate in Fig. 2g. These results (Figs. 2g, 3d) suggest a dominant involvement of CA-mediated H^+

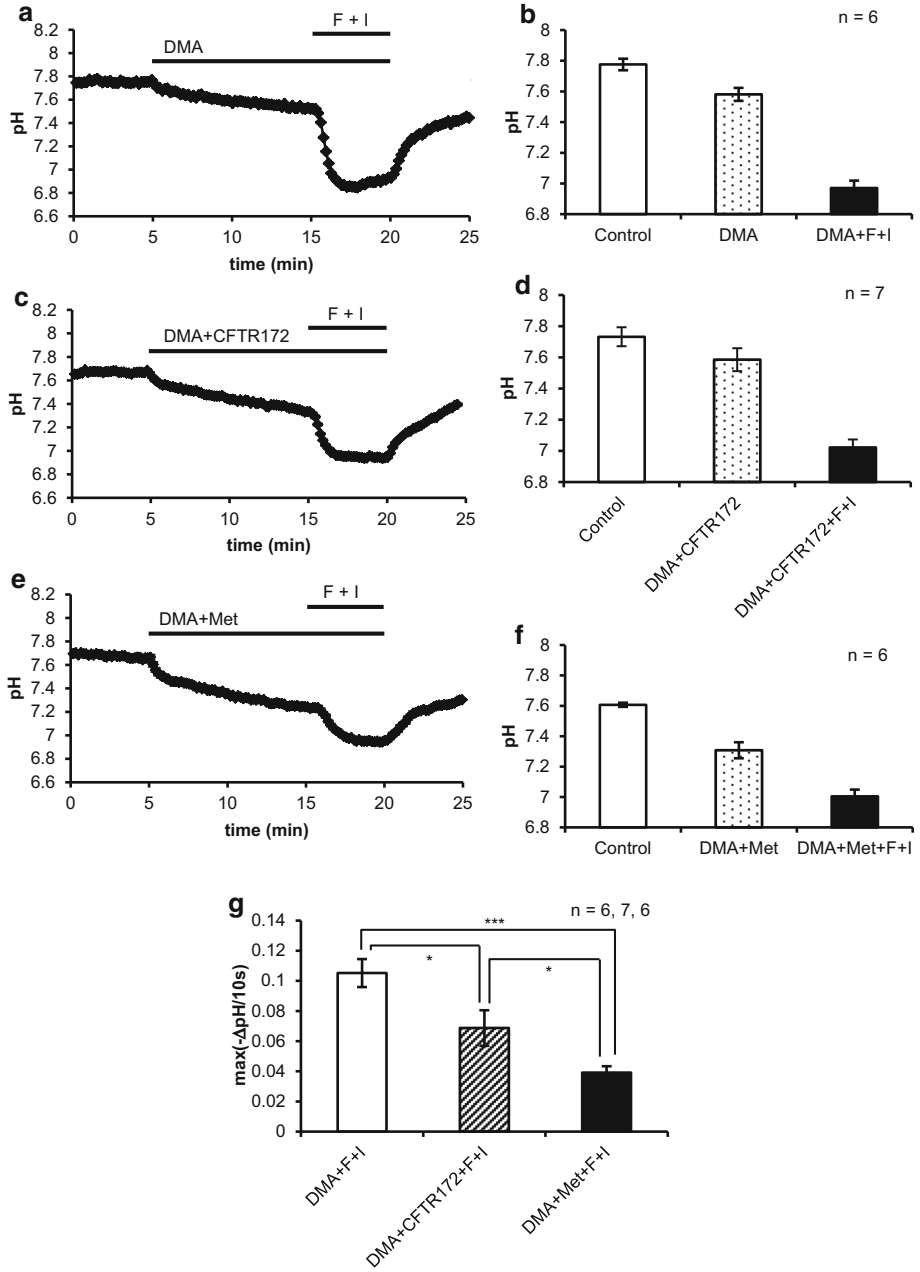

Fig. 2 Effects of 5(*N*,*N*)-dimethyl amiloride (DMA) and its combination with CFTR inhibitor 172 (CFTR172) or methazolamide on forskolin + IBMX (F+I)-induced pH_i changes. **a** A time course of pH_i change during the applications of DMA and DMA + forskolin + IBMX. The pH_i was decreased by the addition of 20 μM DMA and further decreased by the subsequent addition of 10 μM forskolin + 100 μM IBMX (F+I). Each *point* indicates the mean ± SE of pH_i in 19 regions of the duct. **b** The pH_i averages for 1 min just before (control) and 9–10 min after DMA addition (DMA), and 4–5 min after the subsequent addition of F+I (DMA + F+I). Data shown are mean ± SE ($n = 6$). **c** A representative trace of pH_i change during the applications of DMA + CFTR172 (10 μM) and DMA + CFTR172 + F+I. Each *point* indicates the mean ± SE of pH_i in 13 regions of the duct. **d** The pH_i averages for 1 min just before (control) and 9–10 min after (DMA + CFTR172) the addition of DMA + CFTR inhibitor 172, and 4–5 min after the subsequent F+I addition (DMA + CFTR172 + F+I). Data shown are mean ± SE ($n = 7$). **e** A time course of pH_i change during the applications of DMA + 1 mM methazolamide (DMA + Met) and DMA + Met + F+I. Each *point* indicates the mean ± SE of pH_i in 14 regions of the duct. **f** The pH_i averages for 1 min just before (control) and 9–10 min after (DMA + Met) the addition of DMA + methazolamide, and 4–5 min after the subsequent F+I addition (DMA + Met + F+I). Data shown are mean ± SE ($n = 6$). **g** The maximal rates of F+I-induced decreases in pH_i (−ΔpH per 10 s) in the presence of DMA. Simultaneous addition of CFTR172 with DMA significantly reduced the rate, and the addition of methazolamide reduced the rate more effectively. $^*P < 0.05$, $^{***}P < 0.001$ in the unpaired Student's *t* test. Data shown are mean ± SE ($n = 6$, 7, and 6, respectively)

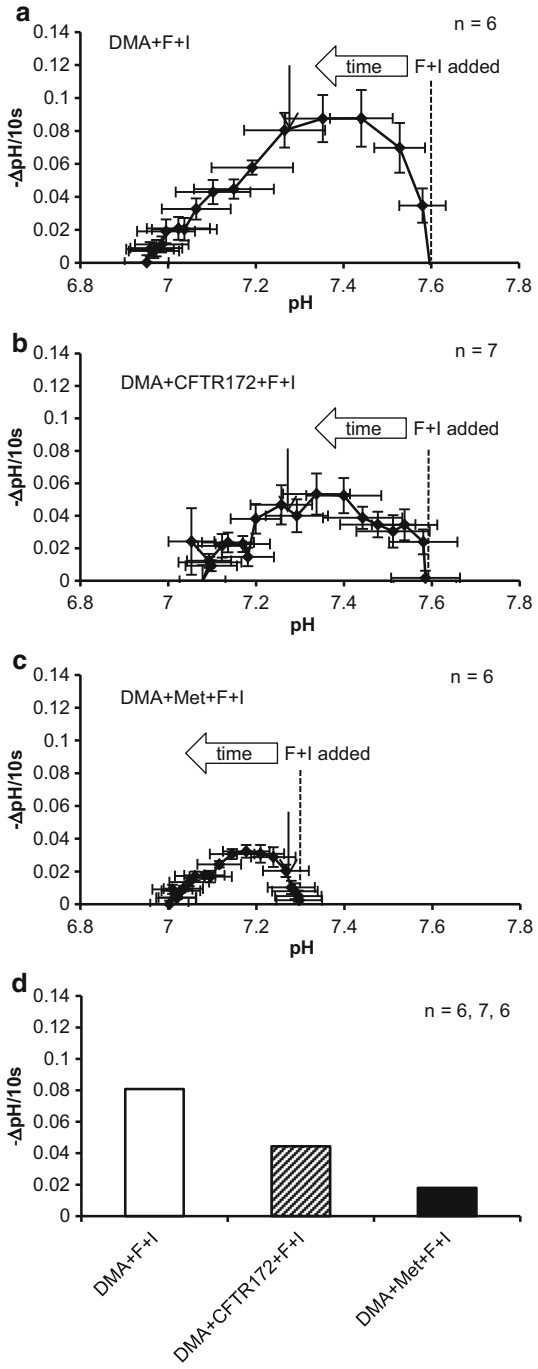

◀**Fig. 3** Evaluation of the contribution of carbonic anhydrases and CFTR Cl^- channels to forskolin + IBMX-induced pH_i changes. **a**–**c** Relationships between the averaged rates of pH_i decreases ($-\Delta pH$ per 10 s) versus the corresponding, averaged pH_i during the pH_i-decreasing phase by 10 μM forskolin + 100 μM IBMX (F+I) stimulation in the presence of 5(*N*,*N*)-dimethyl amiloride (DMA; 20 μM), and its combination with CFTR inhibitor 172 (CFTR172; 10 μM) or methazolamide (Met; 1 mM). The averaged rates of pH_i decreases were plotted at 10 s intervals as the pH_i was decreased by F+I stimulation with the starting point indicated as F+I added. Data shown are mean ± SE ($n = 6$, 7, and 6, respectively). **d** The rates of F+I-induced decreases in pH_i ($-\Delta pH$ per 10 s) at pH_i of 7.27 in the presence of DMA. Simultaneous addition of CFTR172 with DMA reduced the rate, and the addition of methazolamide reduced the rate more effectively ($n = 6$, 7, and 6, respectively). The rate at pH_i 7.27 was obtained by using linear interpolation between two data points of the means, as indicated by an *arrow*, in (**a**–**c**) of each condition

generation rather than CFTR-mediated HCO_3^- release in the F+I-induced decrease in pH_i.

CCh-induced pH_i changes

To study the mechanisms underlying pH_i regulation during HCO_3^- secretion induced by Ca^{2+} signaling, we applied CCh, a Ca^{2+}-mobilizing muscarinic agonist [15, 33]. Figure 4a shows time courses of pH_i changes elicited by the addition of CCh in rat parotid intralobular ducts. Resting pH_i was dispersed between 7.40 and 7.85 ($n = 30$), and the dispersion of pH_i at the steady state of CCh stimulation became smaller mostly to a range between 7.49 and 7.68 ($n = 28$) except two high pH_i data during the stimulation. Altogether, pH_i in 30 ducts (Fig. 4a) changed from 7.63 ± 0.02 to 7.59 ± 0.01 by CCh stimulation on average (mean ± SE, $n = 30$) although CCh mainly lowered pH_i at the steady state (70 % of 30 ducts). Interestingly, some ducts showed two phases of the pH_i change during CCh stimulation: pH_i was transiently increased and then decreased to be lower ($n = 11$) or higher ($n = 5$) than the initial resting level, presumably dependent on faster activation of the pH_i-raising NHE and slower activation of the pH_i-lowering CA and/or Cl^- channels. There was a correlation between CCh-induced ΔpH and the resting pH_i (Fig. 4b). These results indicate that CCh tends to decrease pH_i in the ducts with the high resting pH_i and increase pH_i with the low resting pH_i, in contrast to the F+I-induced responses showing the decreased pH_i in all the ducts. Variability in the resting pH_i of the ducts may be derived from differences in relative expression levels of NHE, CA and Cl^- channels, and in the intracellular Ca^{2+} concentrations in the resting state. CCh stimulation gathered the pH_i level together and maintained it at a higher level in comparison with that during F+I stimulation, suggesting the existence of a certain activity that was stimulated by CCh, but not by F+I, to elevate the pH_i level.

Effects of CA inhibition by methazolamide on the CCh-induced pH_i change

To characterize the contributions of NHE, CA, and Cl^- channels to the pH_i regulation during CCh stimulation, we first addressed whether the CCh-induced changes in pH_i were due to H^+ and HCO_3^- generation by CA. Under the CA inhibition by methazolamide, CCh increased pH_i in all the ducts tested (Fig. 5a, b; $P < 0.01$ in the paired Student's *t* test). This is in contrast with the effect of

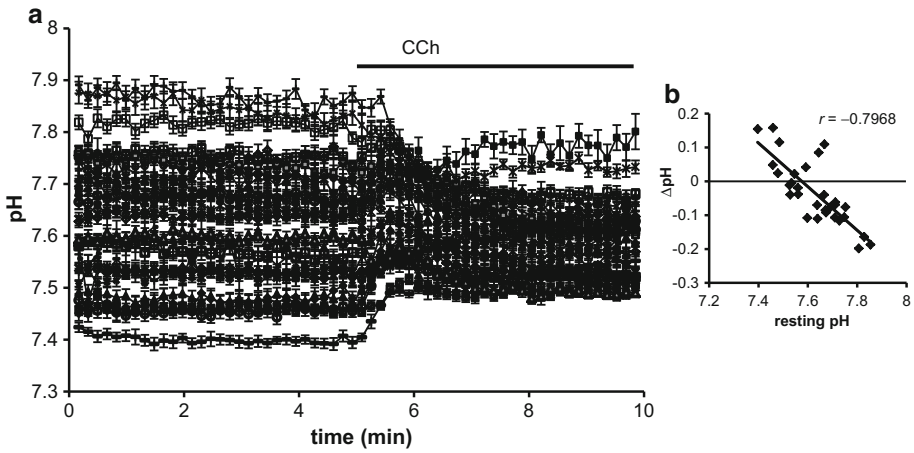

Fig. 4 pH_i changes during the stimulation by 10 μM carbachol (CCh) in rat parotid ducts. **a** Time courses of pH_i changes induced by CCh addition. pH_i dispersion in the resting state became smaller after the addition of CCh. pH_i traces for 30 ducts are shown. **b** Relationships between the CCh-induced pH_i changes (ΔpH) and the resting pH_i levels. Each *point* was obtained from the data in (**a**) ($n = 30$)

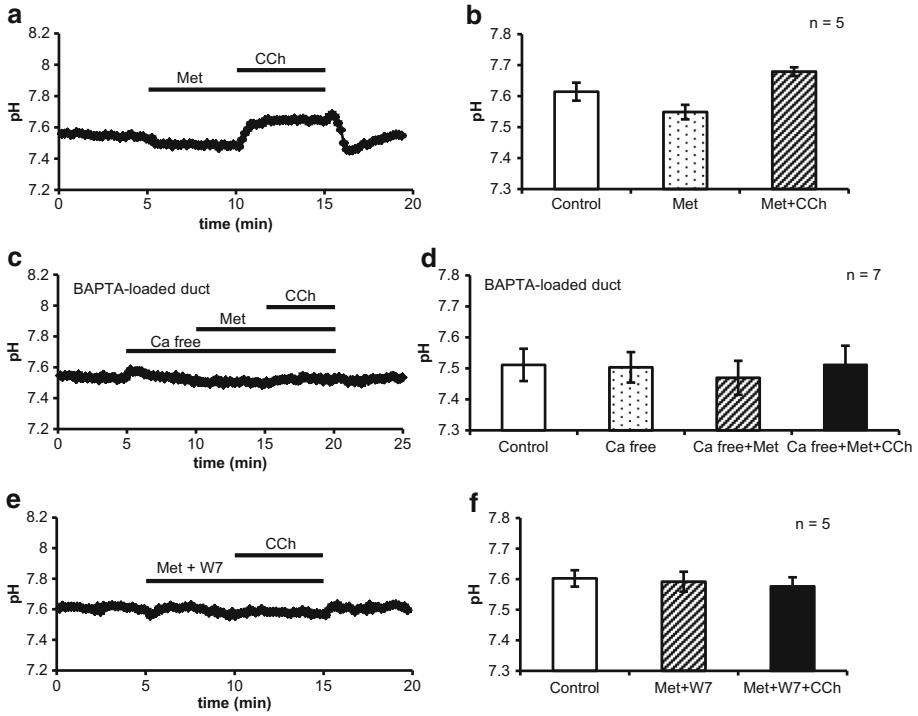

Fig. 5 Effects of blocking H^+ generation by methazolamide, Ca^{2+} chelation and calmodulin inhibition on 10 μM carbachol (CCh)-induced pH_i changes. **a** A time course of CCh-induced pH_i change in the presence of 1 mM methazolamide (Met). CCh evoked an increase in pH_i in all the ducts tested in the presence of methazolamide. Each *point* indicates the mean ± SE of pH_i in 20 regions of the duct. **b** The pH_i averaged for 1 min just before (control) and 4–5 min after (Met) the addition of 1 mM methazolamide and 4–5 min after 10 μM CCh addition (Met + CCh). The pH_i was increased clearly by CCh in the presence of methazolamide. Data shown are mean ± SE ($n = 5$). **c** A representative trace of CCh-induced pH_i change in the absence of the external Ca^{2+} (Ca free) and the presence of 1 mM methazolamide (Met) in the duct loaded with the Ca^{2+}-chelating agent, BAPTA (50 μM BAPTA-AM for 15 min at 37 °C). Each *point* indicates the mean ± SE of pH_i in 18 regions of the duct. **d** Loading BAPTA into the ducts and external Ca^{2+} removal significantly reduced the CCh-induced increase in pH_i, comparing the data shown in **b** (Met + CCh) and **d** (Ca free + Met + CCh) ($P < 0.05$ in the unpaired Student's *t* test, $n = 5$ and 7). The data in **d** are shown as mean ± SE. **e** A time course of CCh-induced pH_i change in the presence of the calmodulin inhibitor, W-7 (W7, 100 μM). Each *point* indicates the mean ± SE in 24 regions of the ducts. **f** W-7 suppressed the CCh-induced increase in pH_i in the presence of 1 mM methazolamide (Met). Data shown are mean ± SE ($n = 5$)

methazolamide on F+I-induced pH changes (Fig. 1d, e). These results suggest not only the presence of CA (some isozymes) activity during CCh stimulation but also that CCh remarkably activates NHE-mediated H^+ extrusion to maintain the higher pH_i, which has been unveiled by inhibiting CA.

Effects of intracellular Ca^{2+} chelation by BAPTA and calmodulin inhibition by W-7 on CCh-induced pH_i changes

To understand the regulatory mechanisms underlying NHE activation during CCh stimulation, we examined whether CCh activated NHE via Ca^{2+}-calmodulin by monitoring the pH_i in the ductal cells under the inhibition of CA. The CCh-induced increase in pH_i in the presence of methazolamide was reduced by extracellular Ca^{2+} removal after intracellular Ca^{2+} chelation by BAPTA (Fig. 5c, d). The effects of Ca^{2+} removal and chelation were significant, comparing the data shown in Fig. 5d (Ca free + Met + CCh) with those in Fig. 5b (Met + CCh) ($P < 0.05$ in the unpaired Student's t test, $n = 7$ and 5). The CCh-induced increase in pH_i in the presence of methazolamide was also significantly suppressed by the calmodulin inhibitor W-7 (Fig. 5e, f). Importantly, our data show that the pH_i level of the experimental condition of Met + W7 + CCh (Fig. 5f) was lower than that of Met + CCh (Fig. 5b) ($P < 0.05$ in the unpaired Student's t test, $n = 5$ and 5). These results suggest that Ca^{2+}-calmodulin is involved in the CCh-induced activation of NHE.

CCh-induced pH_i changes under the inhibition of NHE by DMA

To further characterize the contributions of NHE, CA and Cl^- channels to the pH_i regulation during CCh stimulation, we deduced and analyzed the pH_i changes mediated by CA and Cl^- channel activities under the inhibition of NHE by DMA. DMA significantly decreased pH_i, and the addition of CCh markedly reduced pH_i in the presence of DMA (Fig. 6a, b; pH_i at DMA + CCh was 7.11 ± 0.05, $n = 7$). Thus, inhibition of NHE activity unveiled the pH_i-lowering activities of CA and/or Cl^- channels, enhanced during CCh stimulation. In the presence of the Cl^- channel blocker DPC or methazolamide with DMA, CCh induced a decrease in pH_i to the same level as that during CCh stimulation with DMA alone [Fig. 6c, d (DMA + DPC + CCh); pH_i 7.20 ± 0.08 ($n = 6$), and Fig. 6e, f (DMA + Met + CCh); pH_i 7.15 ± 0.03 ($n = 5$)]. No difference among these three pH_i levels could be due to the lowest limit of pH_i changes during CCh stimulation. Therefore, to evaluate the contributions of CA and Cl^- channel activities to the pH_i changes, we calculated the rate of pH_i change per 10 s, $-\Delta pH/10$ s. The maximal rate of CCh-induced decrease in pH_i in the presence of DMA was shown in Fig. 6g [DMA + CCh; max($-\Delta pH/10$ s) = 0.071 ± 0.003, $n = 7$]. Addition of DPC in the presence of DMA diminished the maximal rate of the CCh-induced pH_i reduction (Fig. 6g), indicating the involvement of Cl^- channel activation in lowering pH_i. Methazolamide also significantly slowed the rate (Fig. 6g), suggesting the contribution of CA activity to the pH_i decrease. Average of $-\Delta pH/10$ s at pH_i of 7.27 was also calculated as is described above: pH_i and $-\Delta pH/10$ s were averaged respectively at each sampling time during CCh stimulation in the ducts (Fig. 7a–c). Figure 7d shows that relative amplitude of the rate in each condition was similar to that of the maximal rate in Fig. 6g. These results (Figs. 6g, 7d) and the CCh-induced pH_i changes in the absence and presence of methazolamide (Figs. 4a, 5a, b) reveal that CCh remarkably activates NHE which keeps the pH_i at around 7.6 against the pH_i-lowering activities, and that the CCh-induced decrease in pH_i is associated with both the HCO_3^- release through DPC-sensitive Cl^- channels and H^+ generation by CA.

Discussion

F+I-induced pH_i changes and activities of CA, CFTR and NHE in parotid intralobular ducts

F+I consistently decreased the pH_i level despite variability in the resting pH_i observed among the ducts (Fig. 1a–c), indicating the dominance of the pH_i-lowering activities of CA and/or CFTR Cl^- channels over the pH_i-raising NHE activity during F+I stimulation. Since the F+I-induced change was suppressed by methazolamide (Fig. 1d, e) as reported in the previous paper [7], we expected that the F+I-induced decrease in pH_i could be due to facilitation of H^+ and HCO_3^- generation by CA and HCO_3^- release through the CFTR Cl^- channel [12]. Unexpectedly, CFTR inhibitor 172 did not significantly affect the F+I-induced pH_i change (Fig. 1c, g). In addition, CFTR inhibitor 172 moderately reduced the rate of the F+I-induced pH_i change in the presence of DMA, while methazolamide more effectively slowed the rate (Figs. 2g, 3d). These suggest that activation of CFTR Cl^- channels during F+I stimulation is not a major rate-limiting step for pH_i regulation, and that some isozymes of CA in salivary ducts would be activated by F+I (Fig. 8) as CAIX in cultured cells is [30]. F+I-induced CA activation may primarily contribute to the pH_i regulation via generation of H^+ and HCO_3^-, while being followed by and concerting with NHE-mediated H^+ extrusion and CFTR-mediated HCO_3^- release to sustain HCO_3^- secretion by the cAMP signal.

Involvement of the pH_i-lowering activities of CA and Cl^- channels in pH_i regulation during CCh stimulation

The CCh-induced decrease in pH_i, observed in the ducts with high resting pH_i, suggests that the pH_i-lowering CA and/or Cl^- channels would be activated during the

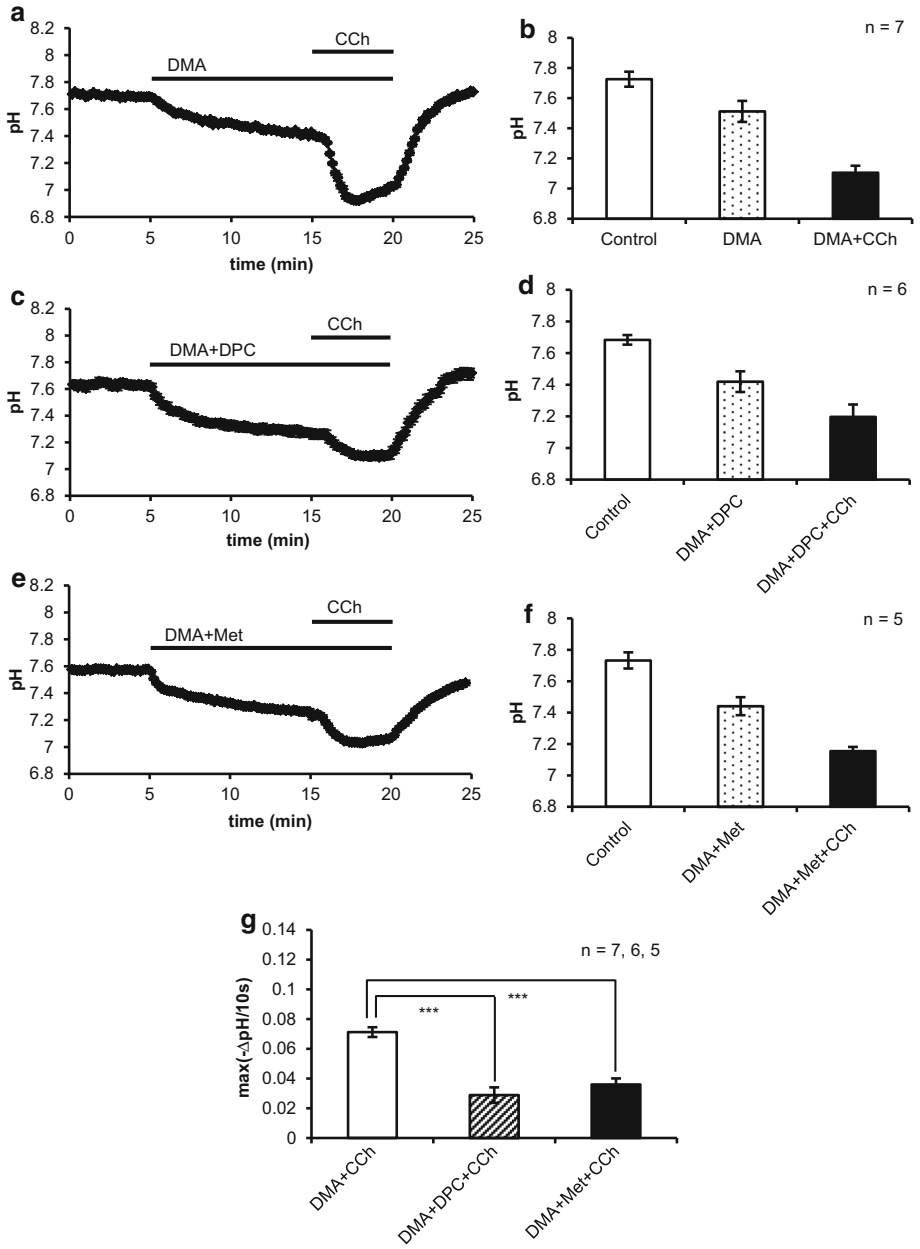

Fig. 6 Effects of 5(*N*,*N*)-dimethyl amiloride (DMA) and its combination with diphenylamine-2-carboxylate (DPC) or methazolamide on carbachol (CCh)-induced pH_i changes. **a** A time course of pH_i change during the applications of DMA and DMA + CCh. The pH_i was decreased by the addition of 20 μM DMA and further decreased by the subsequent addition of 10 μM CCh. Each *point* indicates the mean ± SE of pH_i in 16 regions of the duct. **b** The pH_i averages for 1 min just before (control) and 9–10 min after DMA addition (DMA), and 4–5 min after the subsequent addition of CCh (DMA + CCh). Data shown are mean ± SE ($n = 7$). **c** A representative trace of pH_i change during the applications of DMA + DPC (200 μM) and DMA + DPC + CCh. Each *point* indicates the mean ± SE of pH_i in 17 regions of the duct. **d** The pH_i averages for 1 min just before (control) and 9–10 min after (DMA + DPC) the addition of DMA + DPC, and 4–5 min after the subsequent CCh addition (DMA + DPC + CCh). Data shown are mean ± SE ($n = 6$). **e** A time course of pH_i change during the applications of DMA + 1 mM methazolamide (DMA + Met) and DMA + Met + CCh. Each *point* indicates the mean ± SE of pH_i in 18 regions of the duct. **f** The pH_i averages for 1 min just before (control) and 9–10 min after (DMA + Met) the addition of DMA + methazolamide, and 4–5 min after the subsequent CCh addition (DMA + Met + CCh). Data shown are mean ± SE ($n = 5$). **g** The maximal rates of CCh-induced decreases in pH_i (−ΔpH per 10 s) in the presence of DMA. Simultaneous addition of either DPC or methazolamide with DMA reduced the rate. ***$P < 0.001$ in the unpaired Student's *t* test. Data shown are mean ± SE ($n = 7$, 6, and 5, respectively)

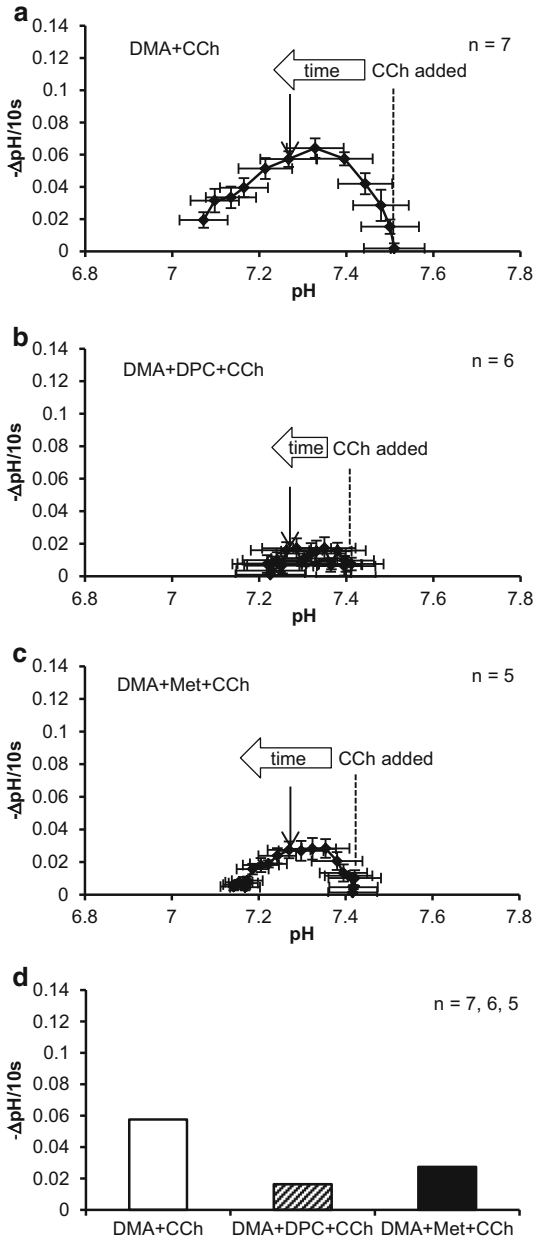

Fig. 7 Evaluation of the contribution of carbonic anhydrases and diphenylamine-2-carboxylate (DPC)-sensitive Cl^- channels to carbachol (CCh)-induced pH_i changes. **a–c** Relationships between the averaged rates of pH_i decreases ($-\Delta pH$ per 10 s) versus the corresponding, averaged pH_i during the pH_i-decreasing phase by 10 μM CCh stimulation in the presence of 5(*N*,*N*)-dimethyl amiloride (DMA; 20 μM), and its combination with 200 μM DPC or methazolamide (Met; 1 mM). The averaged rates of pH_i decreases were plotted at 10-s intervals as the pH_i was decreased by CCh stimulation with the starting point indicated as *CCh added*. Data shown are mean ± SE ($n = 7$, 6, and 5, respectively). **d** The rates of CCh-induced decreases in pH_i ($-\Delta pH$ per 10 s) at pH_i of 7.27 in the presence of DMA. Simultaneous addition of either DPC or methazolamide with DMA reduced the rate ($n = 7$, 6, and 5, respectively). The rate at pH_i of 7.27 was obtained by using linear interpolation between two data points of the means, as is indicated by an *arrow*, in the figure (**a–c**) of each condition

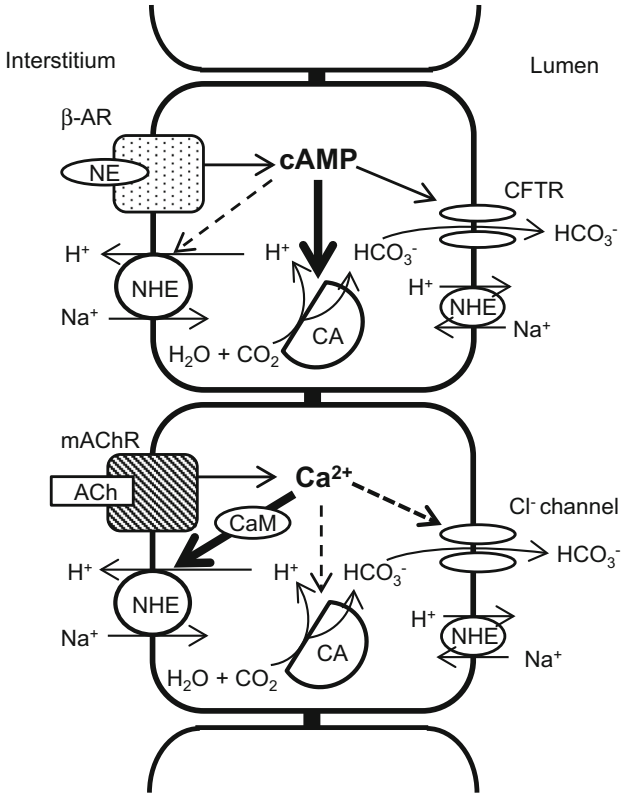

Fig. 8 Schematic illustration for pH_i regulation during HCO_3^- secretion in rat parotid intralobular ducts. Sympathetic β-adrenergic stimulation induces activation of the carbonic anhydrase (CA) rather than the Na^+–H^+ exchanger (NHE), whereas parasympathetic muscarinic stimulation activates NHE on the basolateral membrane at least partially via Ca^{2+}-calmodulin. Both mechanisms facilitate HCO_3^- secretion through the Cl^- channels activated by the stimulations. *Thick arrows* indicate the rate-limiting activation

stimulation. First, we examined the effects of CA inhibition on the CCh-induced pH_i change. In the presence of methazolamide, CCh increased the pH_i level in all the ducts tested (Fig. 5a, b). It is very likely that the inhibition of CA by methazolamide reduced the cytosolic H^+ generation, and unveiled the activity of the NHE-mediated H^+ extrusion during CCh stimulation. This effect and the methazolamide-induced reduction in CCh-induced pH_i change in the presence of DMA (Figs. 6g, 7d) suggest that some isozymes of CA participate in lowering pH_i by generating H^+ and HCO_3^- during CCh stimulation in order to effectively elicit HCO_3^- secretion.

We also examined the effects of Cl^- channel blockage on the pH_i change. Since the molecular identity of Cl^- channels activated by the Ca^{2+} signal has not been clarified yet in rat parotid intralobular ducts [2], we used the non-specific Cl^- channel inhibitor DPC to block CCh or Ca^{2+}-activated Cl^- channels in the present study as reported in the previous papers [6, 15, 34]. Accordingly, DPC slowed the rate of CCh-

induced pH_i reduction in the presence of DMA (Figs. 6g, 7d). These results suggest that the CCh-induced decrease in pH_i is associated with HCO_3^- release via DPC-sensitive Cl^- channels [6] in addition to H^+ generation by CA.

Involvement of CCh-induced NHE activation in pH_i regulation

Although both pH_i-lowering activities of CA and DPC-sensitive Cl^- channels participate in pH_i regulation during CCh stimulation, the prominent features in the pH_i regulation are derived from pH_i-raising activity. First, the pH_i-raising activity of NHE, which was enhanced during CCh stimulation, maintained the pH_i at a higher level, compared with that during F+I stimulation. Second, CA inhibition suppressed the F+I-induced decrease in pH_i to a level close to, but lower than, the resting level, whereas it caused pH_i to increase during CCh stimulation. Thus, the pH_i-raising NHE is prominently activated by CCh.

The two-phase pH_i change in some ducts during CCh stimulation (Fig. 4a) suggests that NHE activation by the agent may be faster than its Cl^- channel activation. In fact, the time to half-maximal responses of CCh-induced increase in pH_i in the presence of methazolamide (0.36 ± 0.05 min, $n = 5$) (Fig. 5a; and other 4 similar data) was much shorter than that of CCh-induced decrease in pH_i in the presence of DMA (1.25 ± 0.07 min, $n = 7$) (Fig. 6a; and other 6 similar data). The NHE activity may promote an initial increase in pH_i via H^+ extrusion, and the Cl^- channel activity may contribute to a delayed decrease by releasing HCO_3^- through the channel in association with H^+ and HCO_3^- generation by CA. The two exceptional data in Fig. 4a may be due to the much higher NHE activity than those of pH_i-lowering CA and Cl^- channels in the CCh-stimulated states. Since pH_i is regulated by cooperative activities of CA, NHE and Cl^- channels, variability in the expression level of each factor may elicit some pH_i differences among the ducts (Fig. 4).

The resting pH_i was decreased after the addition of DMA (Figs. 2a, b, 6a, b), suggesting that NHE would be partially activated before the stimulation, dependent on the resting NHE phosphorylation or resting intracellular Ca^{2+} concentration ($[Ca^{2+}]_i$) [27]. Importantly, CCh more remarkably decreased pH_i in the presence of DMA than it did in the absence of DMA, suggesting that NHE may be more activated by CCh than in the resting level to maintain the pH_i at around 7.6 against the pH_i-lowering activities of CA and Cl^- channels.

Ca^{2+}-calmodulin-mediated activation of NHE

The Ca^{2+} chelator BAPTA and the calmodulin inhibitor W-7 suppressed the NHE-mediated increase in pH_i, induced by CCh under the inhibition of CA by methazolamide. The effect of Ca^{2+} chelation suggests that the CCh-induced increase in $[Ca^{2+}]_i$ may be a primary trigger of NHE activation by CCh, although CCh also activates other signals and the Ca^{2+} signal has a cross-talk with the cAMP signal in salivary gland cells [2, 3]. Removal of external Ca^{2+} also suppresses HCO_3^- secretion from the duct segments in our previous paper [6]. These results indicate that CCh is most likely to activate the NHE at least partially via Ca^{2+}-calmodulin in the parotid ducts (Fig. 8). This is in accord with the previous reports on parotid acinar cells [27] and cultured cells [24, 25]. To keep pH_i at a rather high level (around 7.6) in a steady state during CCh stimulation, the pH_i-raising NHE may be activated the most among the three pH_i regulators. In other words, activation of NHE may be the rate-limiting step for pH_i regulation and HCO_3^- secretion during the CCh stimulation. In the parotid ducts, the high pH_i level maintained by Ca^{2+}-calmodulin-mediated activation of NHE would advance efficient generation of HCO_3^- from CO_2 and H_2O by CA, resulting in an effective increase in HCO_3^- secretion via DPC-sensitive Cl^- channels. From the viewpoint of pH_i regulation, parasympathetic muscarinic stimulation may be more beneficial to HCO_3^- secretion than sympathetic β-adrenergic stimulation.

Conclusion

Taken together, we conclude that F+I may accelerate HCO_3^- secretion by increasing CA activity for HCO_3^- and H^+ generation, rather than activating NHE for H^+ extrusion and the CFTR Cl^- channel for HCO_3^- release, whereas CCh facilitates HCO_3^- secretion mainly through an increase in H^+ extrusion by the Ca^{2+}-calmodulin-mediated activation of NHE, in addition to activation of DPC-sensitive Cl^- channels and CA (Fig. 8). In this paper, we have revealed that different rate-limiting activities of pH_i regulation for HCO_3^- secretion stimulated primarily by cAMP and Ca^{2+} signals exist in the intralobular ducts of rat parotid glands.

Acknowledgments This work was carried out partially at the Analysis Center of Life Science, Natural Science Center for Basic Research and Development, Hiroshima University.

Compliance with ethical standards

Conflict of interest The authors declare that they have no conflict of interest.

Ethical approval All procedures performed in studies involving animals were in accordance with the ethical standards of the institution at which the studies were conducted.

References

1. Cook DI, Van Lennep EW, Roberts ML, Young JA (1994) Secretion by the major salivary glands. In: Johnson LR (ed) Physiology of the gastrointestinal tract, 3rd edn. Raven Press, New York, pp 1061–1117
2. Lee MG, Ohana E, Park HW, Yang D, Muallem S (2012) Molecular mechanism of pancreatic and salivary gland fluid and HCO_3^- secretion. Physiol Rev 92:39–74
3. Melvin JE, Yule D, Shuttleworth T, Begenisich T (2005) Regulation of fluid and electrolyte secretion in salivary gland acinar cells. Annu Rev Physiol 67:445–469
4. Hirono C, Sugita M, Furuya K, Yamagishi S, Shiba Y (1998) Potentiation by isoproterenol on carbachol-induced K^+ and Cl^- currents and fluid secretion in rat parotid. J Membr Biol 164:197–203
5. Catalán MA, Kondo Y, Peña-Munzenmayer G, Jaramillo Y, Liu F, Choi S, Crandall E, Borok Z, Flodby P, Shull GE, Melvin JE (2015) A fluid secretion pathway unmasked by acinar-specific Tmem16A gene ablation in the adult mouse salivary gland. Proc Natl Acad Sci USA 112:2263–2268
6. Nakamoto T, Shiba Y, Hirono C, Sugita M, Takemoto K, Iwasa Y, Akagawa Y (2002) Carbachol-induced fluid movement through methazolamide-sensitive bicarbonate production in rat parotid intralobular ducts: quantitative analysis of fluorescence images using fluorescent dye sulforhodamine under a confocal laser scanning microscope. Eur J Cell Biol 81:497–504
7. Nakamoto T, Hirono C, Sugita M, Takemoto K, Iwasa Y, Akagawa Y, Shiba Y (2002) Forskolin-induced clearance of the fluorescent dye sulforhodamine from rat parotid intralobular duct lumen: visualization of the secretory function under a confocal laser scanning microscope. J Membr Biol 190:189–196
8. Chaturapanich G, Ishibashi H, Dinudom A, Young JA, Cook DI (1997) H^+ transporters in the main excretory duct of the mouse mandibular salivary gland. J Physiol 503:583–598
9. Li J, Koo NY, Cho IH, Kwon TH, Choi SY, Lee SJ, Oh SB, Kim JS, Park K (2006) Expression of the Na^+–HCO_3^- cotransporter and its role in pH_i regulation in guinea pig salivary glands. Am J Physiol Gastrointest Liver Physiol 291:G1031–G1040
10. Melvin JE (1999) Chloride channels and salivary gland function. Crit Rev Oral Biol Med 10:199–209
11. Martin CJ, Young JA (1971) A microperfusion investigation of the effects of a sympathomimetic and a parasympathomimetic drug on water and electrolyte fluxes in the main duct of the rat submaxillary gland. Pflugers Arch 327:303–323
12. Hirono C, Nakamoto T, Sugita M, Iwasa Y, Akagawa Y, Shiba Y (2001) Gramicidin-perforated patch analysis on HCO_3^- secretion through a forskolin-activated anion channel in rat parotid intralobular duct cells. J Membr Biol 180:11–19
13. Dinudom A, Komwatana P, Young JA, Cook DI (1995) A forskolin-activated Cl^- current in mouse mandibular duct cells. Am J Physiol 268:G806–G812
14. Lee MG, Choi JY, Luo X, Strickland E, Thomas PJ, Muallem S (1999) Cystic fibrosis transmembrane conductance regulator regulates luminal Cl^-/HCO_3^- exchange in mouse submandibular and pancreatic ducts. J Biol Chem 274:14670–14677
15. Ohshima K, Shiba Y, Hirono C, Sugita M, Iwasa Y, Shintani H (2003) Luminal space enlargement by carbachol in rat parotid intralobular ducts. Eur J Oral Sci 111:405–409
16. Evans RL, Bell SM, Schultheis PJ, Shull GE, Melvin JE (1999) Targeted disruption of the Nhe1 gene prevents muscarinic agonist-induced up-regulation of Na^+/H^+ exchange in mouse parotid acinar cells. J Biol Chem 274:29025–29030
17. Nguyen HV, Shull GE, Melvin JE (2000) Muscarinic receptor-induced acidification in sublingual mucous acinar cells: loss of pH recovery in Na^+–H^+ exchanger-1 deficient mice. J Physiol 523:139–146
18. Park K, Olschowka JA, Richardson LA, Bookstein C, Chang EB, Melvin JE (1999) Expression of multiple Na^+/H^+ exchanger isoforms in rat parotid acinar and ductal cells. Am J Physiol 276:G470–G478
19. Park K, Evans RL, Watson GE, Nehrke K, Richardson L, Bell SM, Schultheis PJ, Hand AR, Shull GE, Melvin JE (2001) Defective fluid secretion and NaCl absorption in the parotid glands of Na^+/H^+ exchanger-deficient mice. J Biol Chem 276:27042–27050
20. Yun CHC, Oh S, Zizak M, Steplock D, Tsao S, Tse CM, Weinman EJ, Donowitz M (1997) cAMP-mediated inhibition of the epithelial brush border Na^+/H^+ exchanger, NHE3, requires an associated regulatory protein. Proc Natl Acad Sci USA 94:3010–3015
21. Lee MG, Schultheis PJ, Yan M, Shull GE, Bookstein C, Chang E, Tse M, Donowitz M, Park K, Muallem S (1998) Membrane-limited expression and regulation of Na^+–H^+ exchanger isoforms by P_2 receptors in the rat submandibular gland duct. J Physiol 513:341–357
22. Heming TA, Bidani A (1995) Na^+–H^+ exchange in resident alveolar macrophages: activation by osmotic cell shrinkage. J Leukoc Biol 57:609–616
23. van Borren MMGJ, Baartscheer A, Wilders R, Ravesloot JH (2004) NHE-1 and NBC during pseudo-ischemia/reperfusion in rabbit ventricular myocytes. J Mol Cell Cardiol 37:567–577
24. Wakabayashi S, Bertrand B, Ikeda T, Pouysségur J, Shigekawa M (1994) Mutation of calmodulin-binding site renders the Na^+/H^+ exchanger (NHE1) highly H^+-sensitive and Ca^{2+} regulation-defective. J Biol Chem 269:13710–13715
25. Wakabayashi S, Ikeda T, Iwamoto T, Pouysségur J, Shigekawa M (1997) Calmodulin-binding autoinhibitory domain controls "pH-sensing" in the Na^+/H^+ exchanger NHE1 through sequence-specific interaction. Biochemistry 36:12854–12861
26. Moor AN, Fliegel L (1999) Protein kinase-mediated regulation of the Na^+/H^+ exchanger in the rat myocardium by mitogen-activated protein kinase-dependent pathways. J Biol Chem 274:22985–22992
27. Robertson MA, Woodside M, Foskett JK, Orlowski J, Grinstein S (1997) Muscarinic agonists induce phosphorylation-independent activation of the NHE-1 isoform of the Na^+/H^+ antiporter in salivary acinar cells. J Biol Chem 272:287–294
28. Ogawa Y, Fernley RT, Ito R, Ijuhin N (1998) Immunohistochemistry of carbonic anhydrase isozymes VI and II during development of the rat salivary glands. Histochem Cell Biol 110:81–88
29. Peagler FD, Redman RS, McNutt RL, Kruse DH, Johansson I (1998) Enzyme histochemical and immunohistochemical localization of carbonic anhydrase as a marker of ductal differentiation in the developing rat parotid gland. Anat Rec 250:190–198
30. Ditte P, Dequiedt F, Svastova E, Hulikova A, Ohradanova-Repic A, Zatovicova M, Csaderova L, Kopacek J, Supuran CT, Pastorekova S, Pastorek J (2011) Phosphorylation of carbonic anhydrase IX controls its ability to mediate extracellular acidification in hypoxic tumors. Cancer Res 71:7558–7567
31. Shintani T, Hirono C, Sugita M, Iwasa Y, Shiba Y (2008) Suppression of carbachol-induced oscillatory Cl^- secretion by forskolin in rat parotid and submandibular acinar cells. Am J Physiol Gastrointest Liver Physiol 294:G738–G747
32. Ma T, Thiagarajah JR, Yang H, Sonawane ND, Folli C, Galietta LJV, Verkman AS (2002) Thiazolidinone CFTR inhibitor iden-

tified by high-throughput screening blocks cholera toxin-induced intestinal fluid secretion. J Clin Invest 110:1651–1658
33. Shitara A, Tanimura A, Nezu A, Morita T, Tojyo Y (2007) Multiphoton microscopic imaging of rat parotid ducts demonstrates cellular heterogeneity in Ca^{2+} responsiveness. Arch Oral Biol 52:1072–1078
34. Zeng W, Lee MG, Muallem S (1997) Membrane-specific regulation of Cl^{-} channels by purinergic receptors in rat submandibular gland acinar and duct cells. J Biol Chem 272:32956–32965